Appl Biochem Biotechnol (2009) 159:54–64
DOI 10.1007/s12010-008-8464-0

Application of Quartz Crystal Nanobalance for Simultaneous Determination of Vanillylmandelic and Homovanillic Acids by a Net Analyte Signal-Based Method

Maryam Shojaei · Abdolreza Mirmohseni · Yadollah Omidi · Maryam Farbodi

Received: 23 July 2008 / Accepted: 2 December 2008 /
Published online: 17 December 2008

Abstract Homovanillic acid (HVA) and vanillylmandelic acid (VMA) were selectively determined by quartz crystal nanobalance sensor in conjunction with net analyte signal (NAS)-based method called HLA/GO. An orthogonal design was applied for the formation of calibration and prediction sets including HVA, VMA, and some common and structurally similar urine compounds. The selection of the optimal time range involved the calculation of the NAS regression plot in any considered time window for each test sample. The searching of a region with maximum linearity of NAS regression plot (minimum error indicator) and minimum of predicted error sum of squares value was carried out by applying a moving window strategy. Based on the obtained results, the differences on the adsorption profiles in the time range between 1 and 300 s were used to determine mixtures of compounds by HLA/GO method. Several figures of merit like selectivity, sensitivity, analytical sensitivity, and limit of detection were calculated for both compounds. The results showed that the method was successfully applied for the determination of VMA and HVA.

M. Shojaei (✉)
Department of Natural Sciences, Faculty of Animal Sciences, University of Tabriz, Tabriz, Iran
e-mail: mshojaei@tabrizu.ac.ir

A. Mirmohseni · M. Farbodi
Polymer Research Technology Laboratory, Department of Applied Chemistry, Faculty of Chemistry, University of Tabriz, Tabriz, Iran

A. Mirmohseni
e-mail: mirmohseni@tabrizu.ac.ir

M. Farbodi
e-mail: farbodi@tabrizu.ac.ir

Y. Omidi
Research Center for Pharmaceutical Nanotechnology, Tabriz University of Medical Sciences, Tabriz, Iran
e-mail: yomidi@yahoo.com

Keywords Quartz crystal nanobalance · Net analyte signal · Homovanillic acid · Vanillylmandelic acid · HLA/GO method

Introduction

Urinary homovanillic (4-hydroxy-3-jnethoxyphenylacetic) acid (HVA) and vanillylmandelic (4-hydroxy-3-methoxymandelic) acid (VMA) are quantitatively the most important catabolic products of catecholamines. Increased levels of these metabolites in urine clinically may indicate presence of malignant tumors arising from cells of the neural crest such as neuroblastoma and pheochromocytoma [1–3]. Identification and detection of the abnormal levels of these metabolites in urine samples are necessary to diagnosis and therapy of these pathologies.

A colorimetric method, based on the oxidation of VMA to vanillin, was often used in the clinical laboratories for analysis of VMA. This method is generally free from interferences but involves many lengthy steps of extraction [4].

High-performance liquid chromatography methods have been devised to measure VMA and VMA levels, but developed methods have disadvantages, which include sample pretreatment difficulties, low resolution, slow separation, and large injection volume [5]. The limit of detection of the method was 0.12 mg L^{-1} for VMA with a fluorometric detector [6].

A capillary zone electrophoresis method has been described for HVA and VMA measurement in infant urine samples. In addition to pretreatment process, a concentration step is also necessary with this method, since the concentration in the urine samples of healthy infants is less than the detection limit [7]. Their limits of detection for HVA and VMA were 73.76 and 35.67 mg L^{-1}, respectively.

Recently, a method based on capillary gas chromatography with flame ionization detection was developed for routine analysis of human urine to detect VMA and HVA. In this methodology, an internal standard is used, and the procedure involves ethyl ester formation without isolation of the compounds of interest. However, these instruments are prohibitively expensive [8].

Mass screening emergency for neuroblastoma in childhood demands to develop simple and inexpensive methods with a rapid and quantitative response. Quartz crystal nanobalance (QCN) is a sensing system based on the sorption of analyte on an adsorbent material [9]. The QCN comprises a thin vibrating AT-cut quartz wafer sandwiched between two metal excitation electrodes. When small amounts of mass are adsorbed at the quartz electrode surface, the frequency of the quartz is changed according to the well-known Sauerbrey equation [10]:

$$\Delta F = -2.26 \times 10^{-6} F_0^2 \left(\frac{\Delta m}{A} \right) \tag{1}$$

where ΔF is the measured frequency shift, F_0 the original oscillation frequency of the dry crystal, Δm the mass change, and A the piezoelectrically active area of the excitation electrodes.

Due to some advantages including low cost, portability, and easy on-line analysis, the QCN sensor is extensively used for the measurements of mass changes in a variety of chemical and biological studies, such as determination of volatile organic compounds [11, 12] and poisonous compounds [13] and immunoassay [14, 15].

In some cases, the major drawback of the sensors based on QCN is the lack of selectivity, since along with the analyte, other compounds usually interfere. In other words, there is no discrimination between the sources of the mass changes. To overcome this shortcoming, one approach is the pattern recognition technique, which can be used for the data processing of the QCN signals for the simultaneous determination of mixtures of compounds. Multilinear regression, partial least squares, and net analyte signal (NAS) are examples of multivariate analytical techniques [16–18]. The NAS for any analyte based on spectroscopic methods is that a part of the spectrum from analyte that is orthogonal to the space, spanned by the spectra of all constituents except the analyte. Since the NAS vector indicates a direction only affected by changes in the analyte concentration, it can serve as a fully selective determination of analyte. Therefore, it can be expected identification of different chemicals from interferences [19].

The hybrid linear analysis presented by Goicoechea and Olivieri (HLA/GO) algorithm, one of the NAS-based methods, has been successfully used for resolving multicomponent mixtures. Goicoechea and Olivieri [20] have determined tetracycline in blood serum by using synchronous spectrofluorimetry through the HLA/GO algorithm. This algorithm has also been applied for the simultaneous determination of leucovorin and methotrexate, by spectrophotometric [21] and sorbic and benzoic acids in fruit juice samples by using spectroscopic signals [22]. HLA/GO has also been applied to the determination of binary mixtures of amoxycillin and clavulanic acid by stopped-flow kinetic analysis [23].

To our knowledge, no study reported for the detection and determination of VMA and HVA using QCN technique. In the present study, we report the simultaneous determination of VMA and HVA in the solution containing some common urine analytes using polymethylmetacrylate (PMMA)-coated QCN. NAS is utilized to process the frequency data of the crystal at various times, based on different adsorption dynamics of VMA and HVA on the PMMA-coated QCN.

Theory

Notation

An $I\times J$ data matrix R composed of the calibration responses of I samples at J times, a $J\times 1$ vector s_k containing the pure adsorption profile of analyte k at unit concentration, and an $I\times 1$ vector c_k of calibration concentrations of analyte k are the used matrices and vectors throughout the present work. The NAS for analyte k (r_k^*) is given by the following equation:

$$r_k^* = \left[I - R_{-k}(R_{-k})^{+}\right]r = P_{\mathrm{NAS},k}r \tag{2}$$

where r is the adsorption profile of a given sample (when r is the profile s_k of pure k at unit concentration, Eq. 2 becomes $s_k^* = P_{NAS,k,}s_k$), I is a $J\times J$ unitary matrix, R_{-k} is a $J\times A$ column space spanned by the adsorption profile of all other analytes except k (R_{-k}^{+} is the pseudoinverse of R_{-k} and A is the number of factors used to build the model), and $P_{\mathrm{NAS},k}$ is a $J\times J$ projection matrix which projects a given vector onto the NAS space.

The concentration of component k in an unknown sample is obtained from its adsorption profile (r) as

$$c_k = \frac{s_k^T \mathrm{Pr}}{s_k^T P s_k} = \frac{s_k^T P \mathrm{Pr}}{s_k^T P P s_k} = \frac{\left(s_k^*\right)^T r_k^*}{\left\|s_k^*\right\|^2} \tag{3}$$

The applied method in this research involves using the mean (uncentered) calibration profile. It is first obtained as

$$\overline{r}_{\text{cal}} = \frac{1}{I}\sum_{i=1}^{I} r_{i,\text{cal}} \tag{4}$$

where $r_{i,\text{cal}}$ is the profile for the ith calibration sample. Then, the contribution of analyte k is subtracted from the data matrix R in the following way:

$$R_{-k} = R - \frac{c_k \overline{r}_{\text{cal}}^{T}}{\overline{c}_{k,\text{cal}}} \tag{5}$$

where $\overline{c}_{k,\text{cal}}$ is the mean (uncentered) calibration concentration of analyte k. The calculation of net sensitivity (s_k^*) is then carried out with the following equation:

$$s_k^* = P_{NAS,k}\left[\frac{\overline{r}_{\text{cal}}^{T}}{\overline{c}_{k,\text{cal}}}\right] \tag{6}$$

Selection of Time Window

In the present work, the selection of the optimum range of time window was made by calculating an error indicator (EI) as a function of a moving window for each prediction sample, using information of the net analyte signal regression plot (NASRP). NASRP is a plot of the elements of the sample vector r_k^* versus those of s_k^* and should fit a straight line through the origin, with random residuals and slope c_k. Large and correlated residuals in this plot reveal discrepancies between the measured profile (and thus in r_k^*) and the model and, possibly, bias in the estimated concentration. The expression for EI used in the present context is [23]:

$$\text{EI} = \frac{\left[s^2\left(1 + \frac{N^2 s^2}{4\|r^*\|^2}\right)\right]^{1/2}}{\|r^*\|} \tag{7}$$

where s is the standard deviation from the best-fitted straight line to the NASRP (in a given adsorption region), and N is the number of points in the latter plot.

Figures of Merit

Figures of merit have been used in the literature to study the quality of a given analytical method. The ratio of the magnitude of the NAS vector, which is constructed to be free of interference, to the magnitude of the pure component vector yields the selectivity (SEL). Consequently, selectivity ranges between zero (complete overlap) and unity (no overlap). SEL can be calculated with the following equation [24]:

$$\text{SEL} = \frac{\|s^*\|}{\|s\|} \tag{8}$$

where $\|s^*\|$ is the norm of net sensitivity vector of the I analyte of interest, and $\|s\|$ the norm of total adsorption profile of the sample.

The sensitivity indicates to what extent the response due to a particular analyte varies as a function of its concentration [24] and can be expressed as:

$$\mathrm{SEN} = \left\| s_k^* \right\| \tag{9}$$

The limit of detection has been calculated according to the following expression [23]:

$$\mathrm{LOD} = 3\|\varepsilon\|\|b\| \tag{10}$$

where $\|\varepsilon\|$ is a measure of the instrumental noise. The instrumental noise was calculated by recording five adsorption profiles for blank samples, calculating the norm of the NAS for each sample and the corresponding standard deviation. Finally, the analytical sensitivity can be considered as the most useful parameter for method comparison. The analytical sensitivity, γ, which is defined in analogy to univariate calibration as [23]

$$\gamma = \mathrm{SEN}/\delta r \tag{11}$$

where δr is an estimation of the standard deviation of errors and may be approximated to the above-mentioned $\|\varepsilon\|$. However, the minimum concentration difference that is statistically discernible by a method can be expressed as $\gamma^{-1}(\gamma^{-1} = 1/\gamma)$.

Materials and Methods

Reagents and Material

All reagents used in this experiment were of analytical grade. VMA, HVA, dopamine (DA), tyrosine (Tyr), uric acid (UA), ascorbic acid (AA), and homogentistic acid (HGA) were from Sigma Chemicals with analytical grade. PMMA was synthesized in the laboratory according to the well-known method [25].

Instrumentation

Ten megahertz AT-cut quartz crystals with gold coating on both sides were commercially available from the International Crystal Manufacturer (Oklahoma, USA). For QCN experiments, a home-made apparatus was used as described in our previous work [26].

Procedures

A solution casting method was used to coat the polymer over the quartz crystal electrode. Using a Hamilton microliter syringe (Hamilton BonaduzAG, Switzerland), 4 μL of PMMA/chloroform solution (0.3%, *w*/*v*) was dropped on top of the gold electrode of the quartz crystal. A thin layer of PMMA was obtained after solvent evaporation.

An orthogonal design was applied for the formation of calibration and prediction sets including HVA, VMA, and some common and structurally similar urine compounds. Orthogonal design is used in order to give the most information from the analytical system by using only a few samples. The calibration and prediction sets were prepared according to four-level orthogonal design.

The concentrations varied in the linear range of each compound (30–250 mg L^{-1} for VMA and HVA and 70–300 mg L^{-1} for HGA and 100–400 mg L^{-1} for DA and AA). All solutions were filtered using a syringe filter (0.2 μm) before injecting to the cell. Milli-Q

water was used to desorb analyte and recover the electrode. All measurements were carried out at room temperature (25°C).

Results and Discussion

Determination of Pure VMA and HVA

The polymer-coated electrode was exposed to a constant concentration of aqueous VMA and HVA solutions (50 mg L^{-1}). Typical responses for VMA are shown in Fig. 1. The frequency of the crystal decreased due to the adsorption of analyte to the surface of polymer-modified electrode according to Eq. 1. The recorded responses showed that the electrode is sensitive to VMA and HVA. The frequency of the crystal was back shifted to its initial value by exposure to the Milli-Q water indicating the full desorption of analyte from the electrode surface (Fig. 1).

As the concentration of analytes (VMA and HVA) increased, the magnitude of the responses increased (Fig. 2). The obtained responses for either of compounds revealed that the response patterns for both are different (Fig. 2). The main difference between VMA and HVA curves appears in the differences of the slopes of the response curves. The response of VMA reaches steady state faster than that of HVA. In other words, the response time of VMA is shorter than HVA response.

The calibration curves were constructed by plotting the frequency shifts against the concentration of VMA and HVA (Fig. 3). The responses were linear against VMA and HVA concentrations in the range 30–250 mg L^{-1} and with linear regression coefficient of 0.9858 and 0.9884 (n=4), respectively.

Determination of VMA in the Presence of Interfering Compounds

Based on the above results, the QCN sensor coated with PMMA can be employed as pure VMA and HVA sensor. Since VMA and HVA are considered as the agents that exist in most urine samples of neuroblastoma patients, it is necessary to investigate the cross-sensitivity between VMA and HVA in the presence of some structurally related urine compounds. Selected urine compounds were AA, DA, Tyr, UA, and HGA, whose frequency shifts were recorded for quartz crystal PMMA-coated electrode upon exposure. The most effecting interfering compounds for the detection of VMA and HVA are AA, DA, and HGA, while no significant interference from Tyr and UA was observed. These two

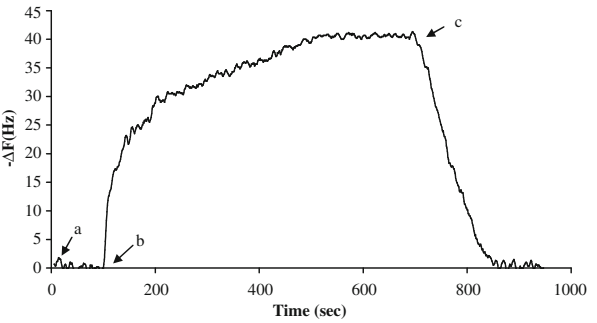

Fig. 1 Typical frequency change of PMMA modified quartz crystal electrode recorded upon exposure to a VMA solution (50 mg L^{-1}). **a** Milli-Q water, **b** VMA solution (50 mg L^{-1}), **c** Milli-Q

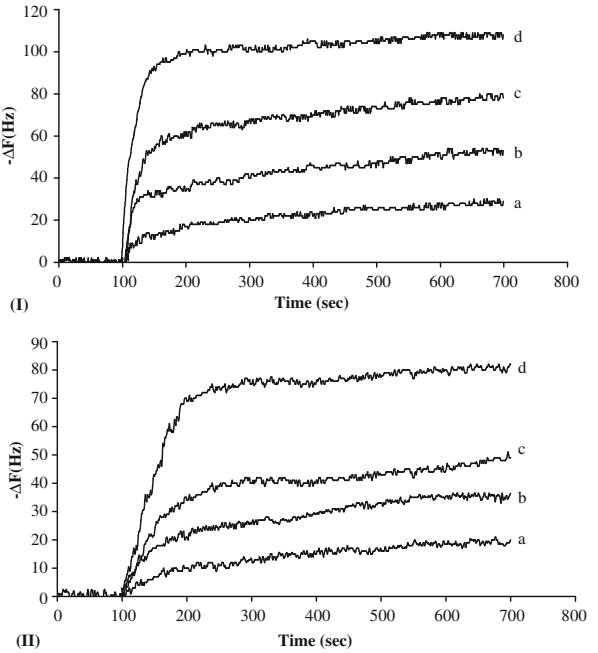

Fig. 2 Frequency changes of PMMA modified quartz crystal electrode as a function of time exposed to various concentration of VMA (*I*) and HVA (*II*) solutions: **a** 30 mg L^{-1}, **b** 75 mg L^{-1}, **c** 150 mg L^{-1}, **d** 250 mg L^{-1}

compounds were present at saturation levels because of their low solubilities in water. The linear ranges were obtained 70–300 mg L^{-1} for HGA and 100–400 mg L^{-1} for DA and AA.

The frequency shift obtained for quartz crystal PMMA-coated electrode upon exposure to a mixture of HAV (50 mg L^{-1})/VMA (70 mg L^{-1})/HGA (90 mg L^{-1})/DA (110 mg L^{-1})/AA (130 mg L^{-1}) were recorded (Fig. 4). The concentrations were selected from the linear range of each compound. The obtained responses showed a significant change in the shape of the frequency–time curves of VMA, including HVA and other interfering compounds (Fig. 4). Then, NAS-based HLA/GO method was considered to develop a model for the selective determination of VMA and HVA in the presence of urine compounds.

Optimization of HLA/GO Method

Selection of the optimum number of factors to be used within the HLA/GO algorithms allows one to model the system with the optimum amount of information. In HLA/GO

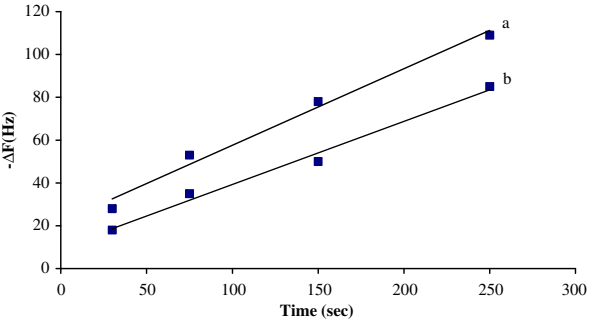

Fig. 3 Calibration graph for VMA and HVA solutions exposed to PMMA modified quartz crystal electrode. Exposure time: 10 min

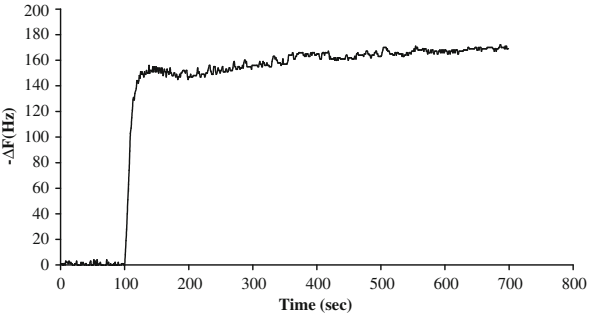

Fig. 4 PMMA modified QCN sensor response upon exposure to a mixture of HVA (50 mg L^{-1})/ VMA(70 mg L^{-1})/HGA | (90 mg L^{-1})/DA (110 mg L^{-1})/ AA (130 mg L^{-1})

analysis of the calibration set, the predicted error sum of squares (PRESS) value for prediction samples varies as a function of the number of factors. In the present work, cross-validation has been used to select the optimum number of factors for several time intervals, in the range comprised between 1 and 600 s.

The selection of the optimum time region caused an increase in the predictive ability of multivariate analysis by discarding the non-informative parts of adsorption profile from the original data. In order to select the most informative range in the adsorption profile, a moving window strategy was applied to the calibration set.

The selection of the optimum time region for the analysis was carried out by evaluating the best predicted values for the prediction samples and the minimum error EI values. In this regard, using the optimized number of factors selected in each region, an EI was calculated for each prediction sample, using information of the NASRP.

The moving window was obtained by varying both the position of the first time and the time range. Table 1 shows the ranges of time tested, the optimum number of factors for each region, the EI values calculated, and the predicted values for VMA and HVA. The minimum EI value calculated using information of the NASRP indicates 1–300 s as the most adequate time region for the analysis in this case.

Usual statistical parameters giving an indication of the quality of fit of all the data are PRESS, square of the correlation coefficient (R^2), and relative error of prediction (REP%). They are respectively defined as:

$$\mathrm{PRESS} = \sum \left(c_{\mathrm{act}} - c_{\mathrm{pred}}\right)^2 \tag{12}$$

Table 1 Optimization of the sensor range in the prediction of VMA and HVA in the mixture by application of the NAS signal and evaluation of the EI.

Sample	Time range	Factor	EI	VMA[1]	VMA[2]	Error	EI	HVA[a]	HVA[b]	Error
1	1–300	7	0.30	60	62.91	2.91	0.30	80	84.79	4.79
	300–600	5	0.34		73.45	13.45	0.34		63.86	−16.14
	1–600	8	0.36		69.5	9.5	0.36		88.36	8.36
2	1–300	7	0.26	140	145.5	5.5	0.26	160	163.06	3.06
	300–600	5	0.17		128.68	−11.32	0.17		137.12	−22.88
	1–600	8	0.14		147.01	7.01	0.14		145.24	−14.76

[a] Actual concentration

[b] Predicted concentration

Table 2 Calibration statistical parameters for VMA and HVA using HLA/GO model.

Statical parameters	VMA	HVA
Time range	1–300	1–300
PRESS	93.51	90.29
REP%	3.89	3.24
R^2	0.9911	0.9921
$\|\|\varepsilon\|\|$	0.36	0.32
Selectivity	0.0088	0.0066
Sensitivity	0.0206	0.0125
γ	0.057	0.034
LOD	44.3	63.8

$$\mathrm{REP} = \left(\frac{100}{\overline{c}}\right)\left[\left(\frac{1}{I}\right)\sum_{1}^{I}\left(c_{\mathrm{act}} - \overline{c}_{\mathrm{pred}}\right)\right]^{1/2} \tag{13}$$

$$R^2 = 1 - \sum_{1}^{I}\left(c_{\mathrm{act}} - c_{\mathrm{pred}}\right)^2 \Bigg/ \sum_{1}^{I}\left(c_{\mathrm{act}} - \overline{c}\right)^2 \tag{14}$$

where $\overline{c}$ is the average component concentration in the I calibration mixtures. The obtained values for the present calibration are summarized in Table 2. Similar statistical parameters are observed for both compounds. The optimized model was tested in the analysis of the prediction set and plots of c_{pred} versus c_{act} were constructed (Fig. 5). As it can be seen, the

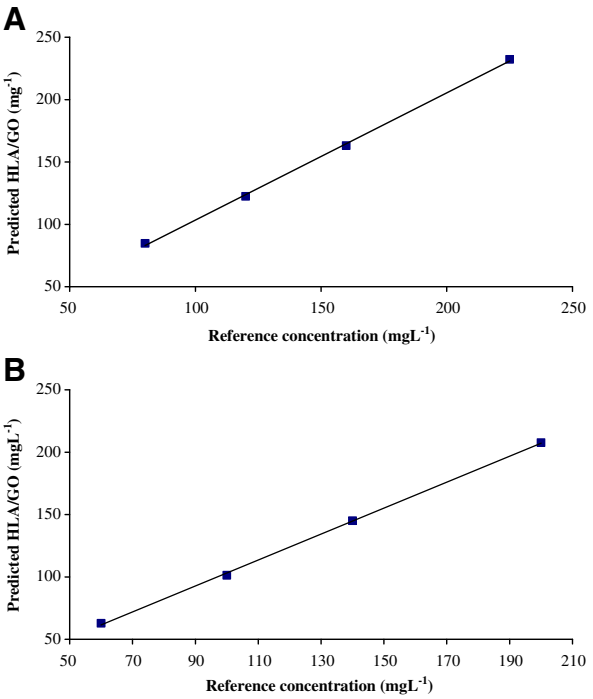

Fig. 5 Predicted versus actual concentrations for HLA/GO calibration models **A** VMA, **B** HVA

plot showed very good linearity, and the values of 0.9982 and 0.9985 were obtained as correlation coefficient for VMA and HVA, respectively.

Figures of Merit

Selectivity, sensitivity, analytical sensitivity, and limit of detection are the most reported figures of merit in the literature to quantify the quality of a given multivariate model. Analysts use these parameters for characterizing, comparing, or developing new analytical methods. HLA/GO allows the estimation of the figures of merit such as selectivity, sensitivity, analytical sensitivity, and limit of detection in the concentration interval assayed. In Table 2, calculated selectivity, sensitivity, $\gamma-1$, and limit of detection for both components through HLA/GO method for VMA and HVA in the samples have been summarized.

The obtained results show the satisfactory performance of the biosensor in simultaneous determination of VMA and HVA. However, this work is the first effort to develop a VMA and HVA biosensor by using QCN in conjunction with HLA/GO method. Therefore, obtained parameters could not be used in comparison studies.

Conclusion

HVA and VMA were simultaneously determined using adsorption profile data recorded using MMA-coated QCN sensor in conjunction with HLA/GO multivariate calibration method. Determination was based on frequency shifts of PMMA-modified quartz crystal electrode due to the adsorption of VMA and HVA at the surface of modified electrode. The responses were linear against VMA and HVA concentrations in the range 30–250 mg L^{-1} and with linear regression coefficient of 0.9858 and 0.9884 (n=4), respectively. The selection of optimum time ranges for each analyte separately were performed by getting the minimum EI, based on the minimization of the PRESS, as a function of a moving adsorption time window. The analysis of the prediction set was used to test the optimized model, and plots of c_{pred} versus c_{act} showed very good linearity. The values of 0.9982 and 0.9985 were obtained as correlation coefficient for VMA and HVA, respectively. REP% of 3.89% and 3.24% were calculated for VMA and HVA, respectively. Several figures of merit such as sensitivity, selectivity, analytical sensitivity, and limit of detection were also calculated.

Acknowledgments We are most grateful for the financial supports of this research project by the University of Tabriz and the Research Center for Pharmaceutical Nanotechnology (RCPN) of Tabriz University of Medical Science.

References

1. Young, J. L., Ries, L. G., Silverber, E., Horm, J. W., & Miller, R. W. (1986). *Cancer*, *58*, 598–602. doi:10.1002/1097-0142(19860715)58:2+<598::AID-CNCR2820581332>3.0.CO;2-C.
2. Schweisguth, O. (1968). *Journal of Pediatric Surgery*, *3*, 118–120. doi:10.1016/0022-3468(68)90993-7.
3. Tuchman, M., Morris, C. L., & Ramnaraine, M. L. (1985). *Pediatrics*, *75*, 324–328.
4. Pisano, J. J., Crout, J. R., & Abraham, D. (1962). *Clinica Chimica Acta*, *7*, 285–291. doi:10.1016/0009-8981(62)90022-0.
5. Radjaipour, M., Raster, H., & Liebich, H. M. (1994). *European Journal of Clinical Chemistry and Clinical Biochemistry*, *32*, 609–613.

6. Anderson, G. M., Feibel, F. C., & Cohen, D. J. (1985). *Clinical Chemistry*, *31*, 819–821.
7. Issaq, H. J., Delviks, K., Janini, G. M., & Muschik, G. M. (1992). *Journal of Liquid Chromatography*, *15*, 3193–3201. doi:10.1080/10826079208020878.
8. Grkovic, S., Nikolic, R., Đordevic, M., & Stojanov, L. (2005). *Indian Journal of Clinical Biochemistry*, *20*, 178–181. doi:10.1007/BF02867423.
9. Lau, K. T., Micklefield, J., & Slater, J. M. (1998). *Sensors and Actuators. B, Chemical*, *50*, 69–79. doi:10.1016/S0925-4005(98)00158-0.
10. Sauerbrey, G. Z. (1959). *Zeitschrift für Physik A Hadrons and Nuclei*, *155*, 206–222. doi:10.1007/BF01337937.
11. Mirmohseni, A., & Oladegaragoze, A. (2004). *Sensors and Actuators B*, *102*, 261–270. doi:10.1016/j.snb.2004.04.027.
12. Mirmohseni, A., & Oladegaragoze, A. (2003). *Sensors and Actuators B*, *89*, 164–172. doi:10.1016/S0925-4005(02)00459-8.
13. Mirmohseni, A., & Alipour, A. (2002). *Sensors and Actuators B*, *84*, 245–251. doi:10.1016/S0925-4005(02)00032-1.
14. Mirmohseni, A. Shojaei, M., & Farbodi, M. (2008). *Biotechnology and Bioprocess Engineering 13,* 592–597.
15. Shojaei, M. Mirmohseni, A., & Farbodi, M. (2008). *Analytical Bioanalytical Chemistry 391*, 2875–2880.
16. Zhu, W., Wei, W., Nie, L., & Yao, S. (1993). *Analytica Chimica Acta*, *282*, 535–541. doi:10.1016/0003-2670(93)80117-4.
17. Nyberg, H. (2008). *Chemometrics and Intelligent Laboratory Systems*, *92*, 118–124. doi:10.1016/j.chemolab.2008.01.002.
18. Mirmohseni, A., Abdollahi, H., & Rostamizadeh, K. (2007). *Analytica Chimica Acta*, *585*, 179–184. doi:10.1016/j.aca.2006.11.082.
19. Lorber, A., Faber, K., & Kowalski, B. R. (1997). *Analytical Chemistry*, *69*, 1620–1626. doi:10.1021/ac960862b.
20. Goicoechea, H. C., & Olivieri, A. C. (1999). *Analytical Chemistry*, *71*, 4361–4368. doi:10.1021/ac990374e.
21. Espinosa-Mansilla, A., Meras, I. D., Gomez, M. J. R., Munoz de la Pena, A., & Salinas, F. (2002). *Talanta*, *58*, 255–263. doi:10.1016/S0039-9140(02)00243-6.
22. Marsili, N. R., Sobrero, M. S., & Goicoechea, H. C. (2003). *Analytical and Bioanalytical Chemistry*, *376*, 126–133.
23. Munoz de la Pena, A., Espinosa-Mansilla, A., Acedo Valenzuela, M. I., Goicoechea, H. C., & Olivieri, A. C. (2002). *Analytica Chimica Acta*, *463*, 75–88. doi:10.1016/S0003-2670(02)00373-2.
24. Goicoechea, H. C., & Olivieri, A. C. (2000). *Trends in Analytical Chemistry*, *19*, 599–605. doi:10.1016/S0165-9936(00)00045-5.
25. Sorenson, W.R. Sweeng, W. Campbell, T.W. (2001). In: *Preparative methods of polymer chemistry, vol. 9*, Wiley, New York, pp. 274–275.
26. Mirmohseni, A., Milani, M., & Hassanzadeh, V. (1999). *Polymer International*, *48*, 873–878. doi:10.1002/(SICI)1097-0126(199909)48:9<873::AID-PI236>3.0.CO;2-W.